https://doi.org/10.5194/egusphere-2025-5783
Preprint. Discussion started: 22 January 2026

Quantifying within-catchment spatial variability of hydrological droughts in cold, humid regions

Gabriel Bastien-Beaudet[1], Marc-André Bourgault[2], Audrey Maheu[1]

[1] Institut des sciences de la forêt tempérée, Université du Québec en Outaouais, Québec, Canada

[2] Département de géographie, Université Laval, Québec, Canada

Corresponding author: Gabriel Bastien-Beaudet (gabriel.bastien-beaudet@uqo.ca)

Abstract

Although catchments serve as the primary unit for water resources management, the spatial distribution of hydrological droughts within catchments remains poorly documented. Many drought assessments rely on sparse gauge networks and presume spatial coherence across the hydrometric network, an assumption that is rarely verified. This study provides one of the first large-scale assessment of within-catchment spatial variability in hydrological droughts, focusing on cold, humid regions. Using 52-year streamflow timeseries of thousands of stream reaches spread across 109 catchments, we examined the duration, severity, and spatial extent of droughts identified with the Standardized Streamflow Index (SSI). Hydrological droughts showed greater within-catchment spatial variability than previously documented: 37% of events were widespread (>90% of the catchment), while 14% were highly localized (<10% of the network). As a result, a single downstream stream gauge would have missed about 30% of drought events within a given catchment, whereas increasing monitoring density to one gauge per 100 km² raised detection rates to nearly 100% in most catchments. The spatial extent of droughts varied significantly with their severity: events spanning over 90% of the network were, on average, twice as severe as those affecting less than 10%. Our findings show that hydrological droughts can be highly variable across hydrometric networks in cold, humid regions, highlighting the importance of integrating spatial variability into drought management and investigating its controlling factors.

Keywords: streamflow drought, within-catchment variability, spatial coherence, spatial extent, drought 32 monitoring, water resources

Highlights:

- 37% of droughts were widespread, affecting >90% of the catchment, while 14% were highly localized, impacting <10% of the network.
- Catchment-wide hydrological droughts are, on average, twice as severe as localized events.
- Using only a stream gauge may fail to detect ~30% of droughts, misrepresenting conditions across the catchment.

https://doi.org/10.5194/egusphere-2025-5783
Preprint. Discussion started: 22 January 2026

1. Introduction

Climate change is intensifying the global water cycle (Allan et al., 2020) and is projected to increase the severity of hydrological droughts (Prudhomme et al., 2014). Hydrological droughts occur when streamflow falls largely below the long-term average in streams or rivers (Van Loon, 2015). When coinciding with low flow periods, such events can disrupt public water supply (Wang *et al* 2022), impair river navigation, cause economic losses in the recreation industry (Wlostowski *et al* 2022) and trigger cascading impacts on water quality (Mosley 2015) and ecosystem health (Bond *et al* 2008). Even outside low-flow periods, hydrological droughts can compromise reservoir reliability (Simeone *et al* 2024) and affect freshwater and riparian organisms whose life cycles are closely tied to the natural flow regime (Lytle and Poff 2004). In regions relying on surface waters for irrigation, hydrological droughts can threaten reservoir storage and food production systems (Lopez-Nicolas *et al* 2017, Pourmahmoud *et al* 2023). Hydrological droughts also pose risks to power generation, limiting hydropower and thermoelectric production due to reduced water availability for cooling (Van Vliet *et al* 2016, Wan *et al* 2021). Given these widespread and diverse impacts, comprehensive, year-round assessments of hydrological droughts, both within and outside of low-flow periods, are essential for evaluating seasonal water availability and guiding water resources management.

Effective drought management requires understanding both the temporal and spatial dynamics of meteorological to hydrological drought propagation. While time lags between meteorological and hydrological droughts have been extensively examined, enabling earlier anticipation of low flows and more timely mitigation, the spatial variability of drought impacts across hydrometric networks remains far less studied. For example, several studies have investigated how meteorological droughts evolve into hydrological droughts, highlighting differences in propagation dynamics between humid and semi-arid climates (Wu *et al* 2024, Zhou *et al* 2024, Bevacqua *et al* 2021). However, few propagation studies explicitly address spatial variability. Evidence from Central Europe suggests that the spatial extent of droughts tends to expand as they propagate from meteorological to hydrological events (Brunner and Chartier-Rescan 2024), highlighting the need to better consider spatial dimensions in drought assessments.

Spatial coherence, or the tendency of hydrological droughts to occur simultaneously across multiple locations, is particularly important for risk management and adaptation planning. For example, in Great Britain, climate change is projected to increase the co-occurrence of droughts across regions, potentially limiting the feasibility of inter-regional water transfers (Tanguy et al., 2023). In Brazil, measures of spatial connectedness revealed that certain regions are more prone to compounding droughts, informing the design of risk-pooling systems (Gesualdo *et al* 2024). Most studies on spatial coherence have focused on large-scale assessments across entire countries or continents (e.g. Great Britain in Hannaford et al., 2011; Iberian Peninsula in Lorenzo-Lacruz et al., 2013; United States in Apurv & Cai., 2020). While valuable for understanding broad drought propagation mechanisms, such studies offer limited insight for catchment-scale water management, where decisions are made based on local streamflow conditions.

In this study, we address this knowledge gap by examining how hydrological drought characteristics—specifically duration and severity—vary within catchments using a highly spatialized streamflow dataset. We hypothesize that severe droughts will exhibit high spatial coherence, affecting the majority (>90%) of the hydrometric network, whereas mild droughts will be more spatially localized, impacting only limited (<10%) portions of the catchment. By focusing on catchment-scale spatial variability, our work provides novel insights into drought dynamics that are directly relevant for local water management and adaptation planning.

https://doi.org/10.5194/egusphere-2025-5783
Preprint. Discussion started: 22 January 2026

2. Methodology

2.1 Study area

This study was conducted in the southern portion of the province of Quebec, Canada (fig. 1). This region is predominantly characterized by a warm-summer humid continental climate (Köppen climate classification Dfb), with areas north of the 50th parallel falling within the subarctic climate zone (Dfc). Across the study area, mean annual air temperatures vary between -4 and 8 °C, with a marked contrast between the cold (mean = -10 °C in winter) and warm season (mean = 23 °C in summer) (MELCCFP, 2012). Mean annual precipitation range from 850 to 1450 mm across the study area, with about 25% falling as snow (Lachance-Cloutier et al., 2017). The study targeted 109 individual unregulated catchments, free of flow regulation from dams. Catchment drainage area ranged from 375 to 21 897 km^2 (median = 2165 km^2) while elevation ranged from 0 to 1339 meters above sea level (median = 382 meters) (NRCan, 2013). Catchment boundaries and characteristics were retrieved from the Quebec Hydrometric Network Geobase (MRNF, 2019), a high-resolution hydrometric dataset.

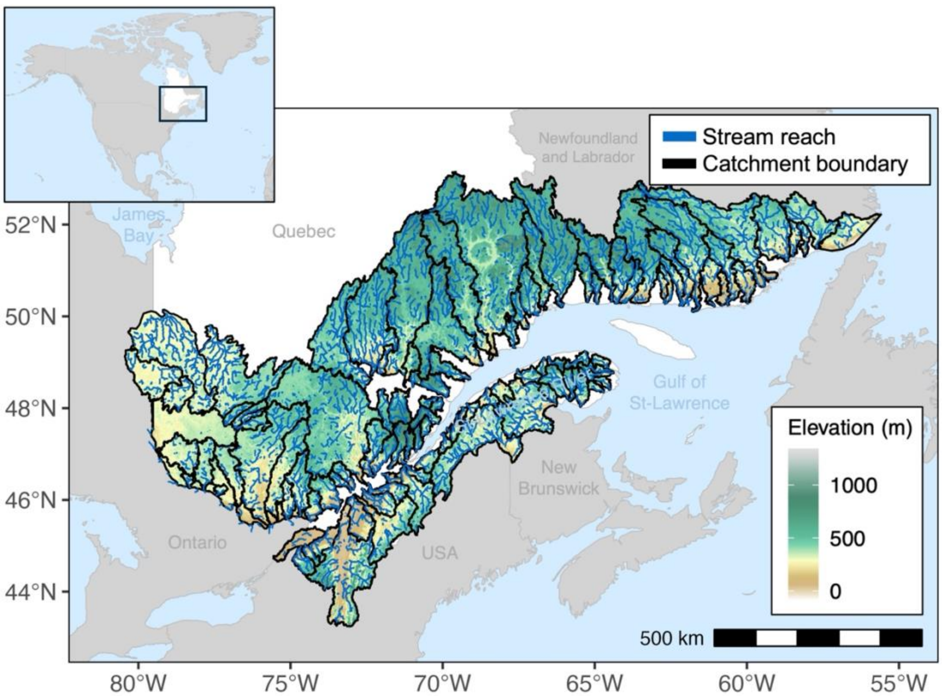

Figure 1. Spatial domain of the study area with the 109 catchment boundaries (black lines) extracted from the Quebec Hydrometric Network Geobase (MRNF, 2019), the stream reaches used in the study (dark green lines) and topography from the Canadian Digital Elevation Model (NRCan, 2013). In certain catchments, fewer stream reaches were considered given that catchment portions regulated by dams were not considered in the study. Additionally, only reaches with a drainage area of 100 km^2 or greater were included due to high uncertainty in reconstructed flows for smaller catchments (MELCCFP, 2018).

https://doi.org/10.5194/egusphere-2025-5783
Preprint. Discussion started: 22 January 2026

2.2 Historical Streamflow dataset

Hydrological droughts were identified using a streamflow dataset from the Hydroclimatological Atlas of Southern Quebec (MELCCFP, 2023) which provides daily flow values from 1970 to 2022 for a dense hydrological network of stream reaches spanning the region of southern Quebec. This dataset was developed in two steps: i) hindcasting using the HYDROTEL semi-distributed hydrological model followed by ii) post-processing with streamflow data assimilation using an optimal interpolation method (Lachance-Cloutier et al., 2017). Details of the two steps are provided below, and additional, comprehensive details on model configuration, calibration procedures, and validation results are provided in Malenfant et al. (2022). This dataset is used operationally by multiple local government entities and private sector companies.

HYDROTEL is a physically based, semi-distributed hydrological model that defines computational units based on land use, soil classification and geographical features (Fortin et al., 2001). For the streamflow reconstruction, daily gridded air temperature and precipitation datasets were created by interpolating observations from ~300 meteorological stations and used as model forcing inputs. A regional calibration (Ricard *et al* 2013) was conducted to optimize average model performance across 70 watersheds, with validation based on 151 stream gauges. Six model configurations were used to capture uncertainty relative to process representation (e.g. choice of evapotranspiration model) and parameter estimation (Malenfant et al., 2022). All configurations demonstrated good performance, with median Kling-Gupta Efficiency (KGE', Kling et al., 2012) ranging between 0.72 and 0.78 (Malenfant et al., 2022).

HYDROTEL model hindcasts were post-processed using optimal interpolation as a data assimilation method. Optimal interpolation aims to improve streamflow estimates by accounting for the spatial correlation of errors (i.e. model deviations from observations) and a detailed description of the method is available in Lachance-Cloutier et al. (2017). Streamflow observations were obtained from 279 stream gauges with minimal influence from hydraulic structures (e.g. dams) and major lakes. The ratio between the variance of the observation error and the variance of the model error was set to 0.25, effectively assigning four times greater weight to observations than to model hindcasts when estimating streamflow at a reach with a nearby stream gauge and no others in close proximity. Error correlation decreased with distance, reaching zero at 200 km. In a case study involving 75 stream gauges across southern Quebec, optimal interpolation outperformed other streamflow reconstruction methods relying solely on observations or model outputs, achieving a KGE' of 0.86 in a leave-one-out cross-validation (Lachance-Cloutier et al., 2017).

From the streamflow reconstruction dataset, the daily median streamflow values were used to assess hydrological droughts. Only reaches with a drainage area of 100 km^2 or greater were included due to high uncertainty in modelled streamflow for smaller catchments (MELCCFP, 2018). Catchments with fewer than 10 reaches with available data were excluded, as such limited spatial coverage precludes meaningful assessment of spatial coherence. In total, the spatial coherence of hydrological droughts was evaluated for 109 catchments, encompassing streamflow estimates for 6718 reaches (fig 1). These catchments had an average reach length of 8.6 km, with streamflow estimates covering on average 51% of each catchment's total hydrometric network length (Table 1).

https://doi.org/10.5194/egusphere-2025-5783
Preprint. Discussion started: 22 January 2026

Table 1. Characteristics of catchments and stream reaches used in this study. Available hydrometric network length per catchment refers to the sum of lengths from stream reaches with available streamflow data in the catchment. Actual hydrometric network length refers to the sum of lengths of all reaches (with and without streamflow data) in the catchment.

Characteristics	Minimum	Mean	Median	Maximum
Catchment drainage area (km^2)	375	4055	2165	21897
Number of reaches per catchment	10	63	36	409
Length of individual stream reaches (km)	0.1	8.6	5.8	96.5
Available hydrometric network length per catchment (km)	40	536	233	3036
Proportion of available hydrometric network length to actual hydrometric network length per catchment (%)	12	51	53	89

2.3 Standardized Streamflow Index

Drought events were identified using the Standardized Streamflow Index (SSI) (Svensson et al., 2017; Lahaa et al., 2017; Barker et al., 2016). The SSI is computed by fitting a statistical probability distribution to monthly streamflow time series of each catchment, then transforming the monthly streamflow values into quantiles of a standard normal distribution (mean zero, standard deviation one). Thus, each SSI value represents the number of standard deviations a monthly streamflow deviates from the long-term average, enabling comparison across time and space. To ensure an optimal fit, eight candidate distributions (2 parameters: gamma, Gumbel, logistic, log-normal, normal, Weibull; 3 parameters: Generalized Extreme Value, Tweedie) were fitted to each monthly time series of each stream reach. The best-fitting distribution was selected using Kuiper's goodness of fit test (Kuiper, 1960), which is equally sensitive at the median and the tails of the distribution, making it appropriate for the analysis of extreme events such as droughts. The Kuiper's test statistic sums the maximum negative (D-) and maximum positive (D+) distances between two cumulative distribution functions and the distribution minimizing this statistic was chosen as best. SSI values were truncated at -5 and 5 to limit uncertainty at distribution extremes (Svensson et al., 2017). The SSI can be calculated over varying accumulation periods by applying a backward-looking moving average on the monthly streamflow data before standardization. In this study, three accumulation periods (1, 3 and 6 months) were considered which are denoted as SSI-1, SSI-3 and SSI-6. The *SCI* package for R (Gudmundson & Stagge, 2014) was used to compute the SSI, in combination with the *tweedie* package (Dunn, 2005).

2.4 Drought event identification and characteristics

Drought events were identified using the widely applied run theory (Yevjevich, 1967). Specifically, a drought event was defined as a period when SSI values were continuously negative (SSI < 0) with at least one month going under a pre-defined threshold (Barker et al., 2016). Threshold values of -1 (moderate), -1.5 (severe) and -2 (extreme) have been suggested by McKee et al., (1993) and are widely used. A threshold of -1.5 was adopted to focus on severe and extreme events, although sensitivity to this threshold was assessed.

First, drought events were identified at the reach-scale and three characteristics were computed for each event: *duration* (number of months with SSI < 0), *severity* (sum of SSI values during an event) and *occurrence* (season of drought onset). Second, droughts were identified at the catchment scale and concurrent reach-scale events were grouped into a single event when they overlapped by at least one month. The median values of duration

https://doi.org/10.5194/egusphere-2025-5783
Preprint. Discussion started: 22 January 2026

and severity across reaches were used to characterize the catchment-scale event. Last, the *spatial extent* of a catchment-scale drought was quantified as the ratio of stream length affected by drought at any point during the event to the total stream length with available data. Droughts were considered as "widespread" when they affected more than 90 % of the hydrometric network and as "localized" when they affected less than 10% of the hydrometric network.

2.5 Statistical modelling of spatial coherence

To address the hypothesis that severe droughts are spatially coherent within a catchment, the relationship between drought characteristics (duration and severity) and their spatial extent was examined. Given the strong correlation between duration and severity ($R^2 = 0.87$), statistical modelling focused exclusively on *severity* as it combines duration and intensity together into a single indicator. A Gaussian linear mixed model with an identity link function was fitted to model drought *severity* as a function of the covariates. Fixed covariates were *spatial extent* and *occurrence* (season of drought onset). To manage the dependency of drought events within individual catchments, *catchment identifier* was used as random intercept. The year of drought onset (*year*) was also used as random intercept to manage hydrological drought severity dependency between catchments. Drought severity was log-transformed (natural logarithm) to stabilize the variance in the model. The model was fitted using the glmmTMB package in R (Brooks et al., 2017).

2.6 Sensitivity of drought occurrence to streamflow monitoring density

The sensitivity of drought occurrence (i.e., the number of drought events) to streamflow monitoring density (i.e., the number of stream reaches used to compute catchment-scale drought events) was assessed within each catchment. This was done by comparing the number of drought events identified at the catchment scale with those identified when only a single stream reach was used. For each of the 109 catchments, it was first assumed that streamflow data were available only at the most downstream reach and the number of severe drought events (SSI < -1.5) was calculated, following the approach described in Section 2.3. The paired values (full network vs. single reach) were then used to evaluate the general tendency toward under- or overestimation of drought occurrence across the study area. To ensure the results were not biased by the use of the most downstream reach, the analysis was repeated by randomly selecting a single reach (without replacement) within each catchment, repeated 100 times. For each catchment, the mean and standard deviation of the paired number of events were calculated to further characterize the variability and tendency of drought occurrence estimates based on single-reach monitoring.

Further analysis was performed to estimate the number of stream gauges (i.e. number of stream reaches used to compute catchment-scale drought events) require to detect all drought events within a catchment. For each catchment, an increasing number of stream reaches (from 1 up to the total number of reaches) was randomly sampled and the number of severe drought events was computed at each step. The drought detection rate was defined as the ratio of drought events detected using a reduced number of reaches to the total number of events detected using all reaches. These detection rates were then analyzed in relation to monitoring density, expressed as the number of reaches per 100 km² of drainage area. To account for the potential influence of catchment size on drought variability, the analysis was conducted separately for meso-scale catchments (drainage area < 2500 km²) and large-scale catchments (drainage area > 2500 km²).

https://doi.org/10.5194/egusphere-2025-5783
Preprint. Discussion started: 22 January 2026

3. Results

All results presented below correspond to the 3-month accumulation period, unless otherwise stated, as analyses conducted for the 1- and 6-month periods yielded similar results and are only presented in the appendix A (Figures A1-A4, Table A1).

3.1 Drought occurrence, duration, severity at the catchment scale

Over the 52-year study period, catchments experienced an average of 26 drought events, corresponding on average to one event every two years (Table 2). Droughts had a mean duration of 8 months and a mean cumulative severity of -8.1, indicating that streamflow was on average one standard deviation below the long-term mean for each month of a drought event. However, longer and more severe events also occurred, with durations of up to 61 months and severity reaching -75. As expected, drought duration and severity were strongly correlated ($R^2 = 0.87$), reflecting the accumulation of deficits over longer events. On average, 61 % of a catchment's hydrometric network experienced droughts conditions during a given event. Overall, drought characteristics were relatively consistent across seasons: duration, severity, and spatial extent were comparable in spring, summer, and fall. In winter, droughts were slightly less severe and with a reduced spatial extent, though the differences were modest.

Table 2. Annual and seasonal characteristics of catchment-scale hydrological drought events. Seasons are defined as: winter = December/January/February, spring = March/April/May, summer = June/July/August, fall = September/October/November. CV corresponds to the coefficient of variation.

Occurrence	Number of droughts per catchment			Duration (months)			Severity (-)			Spatial extent (% of stream length in drought)		
	Median	Mean	CV (%)	Median	Mean	CV (%)	Median	Mean	CV (%)	Median	Mean	CV (%)
All seasons	27	26	19	7	8	69	- 6.6	- 8.1	74	68	61	60
Winter	5	5	40	6	7	78	- 5.3	- 7.0	81	58	57	65
Spring	9	9	35	6	8	68	- 6.6	- 8.1	70	75	63	59
Summer	7	7	34	7	8	68	- 7.1	- 8.3	73	69	62	59
Fall	6	6	41	7	9	65	- 7.0	- 8.7	72	66	60	61

3.2 Spatial extent of drought varies widely across events.

On average, 61% of the hydrometric network length experienced severe drought during a given event, although substantial variability was observed (CV = 60 %, Table 2).. Overall, 37% of events were widespread (affecting > 90 % of the hydrometric network), while 14 % of events were localized (affecting < 10% of the hydrometric network) (fig. 2b).

The threshold used to define drought events (i.e. one month with SSI < -1.5) had a strong influence on their spatial extent, with spatial coherence decreasing as the threshold became more extreme (more negative). For example, applying a moderate threshold (SSI < -1) resulted in strong spatial coherence, with 59 % of events classified as widespread across the catchment (fig. 2a). In contrast, using an extreme threshold (SSI < -2) reduced spatial extent and coherence (fig. 2c), producing a bimodal distribution of spatial coverage. One cluster of events was widespread, although this represented only 14 % of all events, while a larger cluster of events

https://doi.org/10.5194/egusphere-2025-5783
Preprint. Discussion started: 22 January 2026

(29 %) was localized (fig. 2c). This pattern of reduced spatial coherence with more extreme thresholds was consistent across all seasons (fig. 2).

During a given drought event, stream reaches not classified as experiencing drought typically had SSI values well above the selected threshold, with some even showing above-average streamflow, while other parts of the catchment were under drought conditions (fig. 3). For example, when using the severe threshold (SSI < -1.5), 38 % of reaches had SSI values greater than or equal to zero during drought events (fig. 3). More broadly, the majority (80 % to 92 % depending on the threshold) of reaches not experienced drought conditions during a catchment-scale event had SSI values at least 0.5 units above the threshold (fig. 3), indicating a clear distinction from drought conditions. This pattern was consistent across all seasons.

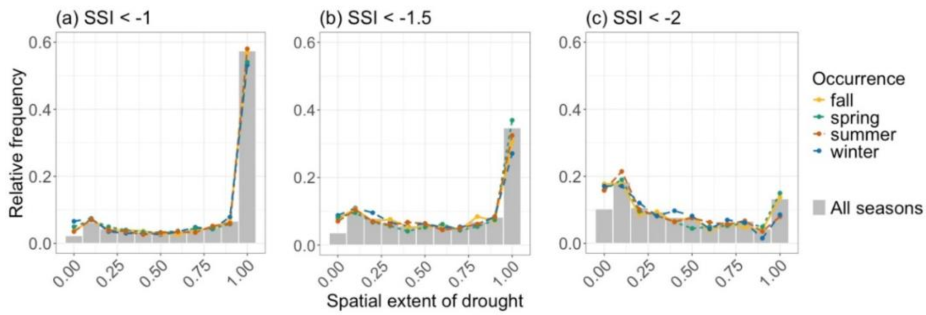

Figure 2. Binned relative frequencies (displayed as both bars and overlaid lines) of the spatial extent of drought events identified with three different thresholds: moderate (SSI < -1), severe (SSI < -1.5) and extreme (SSI < -2). Spatial extent refers to the proportion of the hydrometric network length experiencing drought for a given event. Spatial extent was binned in 11 bins of 0.1 (from 0 to 1) to calculate the relative frequencies of events with different spatial extents. Grey bars represent the entire study area and dotted coloured line refer to the four seasons of drought occurrence (winter = December/January/February, spring = March/April/May, summer = June/July/August, fall = September/October/November).

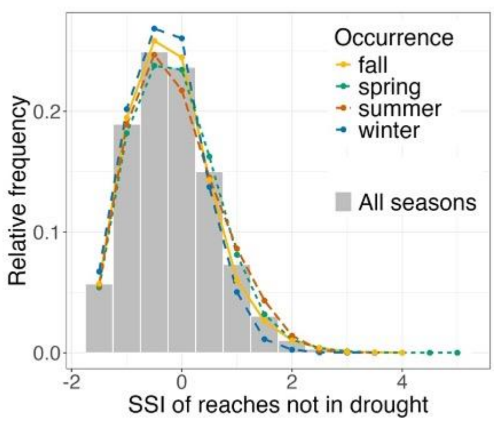

Figure 3. Binned relative frequencies (displayed as both bars and overlaid lines) of the Standardized Streamflow Index (SSI) for reaches that were not experiencing drought during catchment-scale drought events. Drought events were identified with the severe threshold (SSI < -1.5). Indices (SSI) were binned in 14 bins of 0.5 (from -1.5 to 5.0) to calculate the relative frequencies of reaches with different SSI values. Grey bars represent the entire study area and dotted coloured line refer to the four seasons of drought occurrence (winter = December/January/February, spring = March/April/May, summer = June/July/August, fall = September/October/November).

https://doi.org/10.5194/egusphere-2025-5783
Preprint. Discussion started: 22 January 2026

3.3 Catchment-wide hydrological droughts are, on average, twice as severe as localized events.

Results of the linear mixed model showed that the spatial extent of drought events had a significant influence on their severity (Table 3, Figures B1-B3 of appendix B for model validation). Widespread drought events affecting a larger proportion of the hydrometric network tended to be more severe (fig. 4). On average, widespread events (spatial extent > 90%) were nearly twice (1.9 times) as severe as localized events (spatial extent < 10%). Overall, a one-unit increase in spatial extent corresponded to a 2.2-fold ($e^{0.782}$) increase in drought severity. Despite this trend, considerable variability remained, with some highly severe events (severity > 10) occurring even when less than 25% of the catchment was affected (fig. 4). Droughts that began in winter were significantly less severe, while no significant differences in severity were observed among events initiated in spring, summer, or fall (fig. 4, table 3). These patterns held across different thresholds used to define drought events (SSI < -1, -1.5, or -2), although model intercepts increased and slopes decreased with more extreme thresholds (e.g., SSI < -2) (Tables C1-C2, appendix C). The results were also robust to the length of the SSI accumulation period (1, 3, or 6 months; Tables C3-C4, appendix C).

Table 3. Estimated regression parameters, standard errors, z-values, p-values and 95% confidence intervals of the linear mixed model assessing the influence of spatial extent and occurrence on the severity of drought events. Estimated values of variance (σ) for $\sigma_{catchmentID}$ and σ_{year} are 0.018 and 0.031, respectively. Estimated R^2 value is 0.37 (n = 2864).

	Estimate	95% confidence interval	Standard error	z-value	p-value
(Intercept)	1.305	[1.228, 1.384]	0.040	32.78	< 0.001
Spatial extent	0.782	[0.729, 0.835]	0.027	28.86	< 0.001
Occurrence: Fall	0.187	[0.122, 0.251]	0.033	5.70	< 0.001
Occurrence: Spring	0.118	[0.056, 0.180]	0.032	3.71	< 0.001
Occurrence: Summer	0.172	[0.109, 0.234]	0.032	5.36	< 0.001

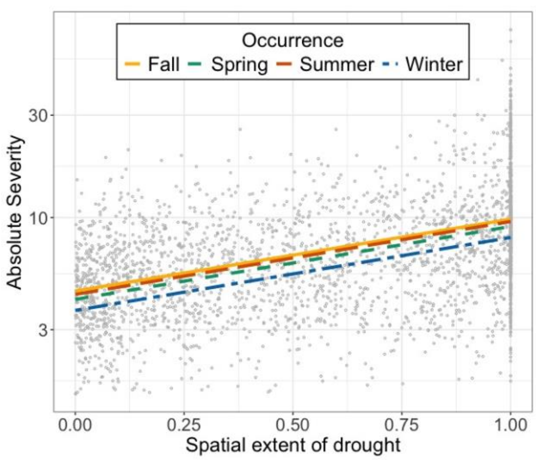

Figure 4. Relationship between the spatial extent of droughts (proportion of the hydrometric network experiencing drought for a given event) and their severity (sum of absolute SSI values during event) across seasons (winter = December/January/February, spring = March/April/May, summer = June/July/August, fall = September/October/November). The severity is represented in log (natural logarithm) scale on the Y axis ($e^1 \sim 3$, $e^2 \sim 10$, $e^3 \sim 30$).

https://doi.org/10.5194/egusphere-2025-5783
Preprint. Discussion started: 22 January 2026

3.4 Relying on a single stream gauge may lead to undetected droughts.

The number of stream reaches experiencing drought within a catchment varied considerably between events (fig. 2), which has important implications when assessing catchment-wide drought conditions with a single stream gauge. To evaluate the potential for underdetection, streamflow data were assumed only available at the most downstream reach of each of the 109 catchments and the number of severe drought events (SSI < -1.5) was computed accordingly (fig. 5a). This approach systematically underestimated the number of events (fig. 3), with an average of 9 events (min = 1, max = 27) per catchment missed, representing an average of 37 % (min = 3 %, max = 78 %) of events going undetected.

On average, two events per catchment (179 events in total) were only detected in a single reach and these events were typically mild, with a median severity of -4.8 (max = -1.5, min = -19.0). Even when excluding these single-reach events, an average of 7 events per catchment remained undetected, corresponding to 30 % (min = 0 %, max = 76 %) of events on average. Using only the most downstream reach to identify drought events led to a decrease in median drought severity from -6.6 (with all reaches) to -7.4 and a decrease in maximum severity from -69.2 to -75.0, suggesting that although undetected events were often mild, some were still highly severe. While fewer drought events were detected at the most downstream reach, the majority of events (60%) detected corresponded to widespread events.

To assess whether this underdetection was specific to the most downstream reach, a resampling analysis was performed by randomly selecting a single reach 100 times for each catchment (fig. 5b). Across all resampling runs, the number of drought events was consistently underestimated compared to results obtained using the full hydrometric network. On average, 35 % (min = 0%, max = 84%) of events went undetected, corresponding to an average of 9 (min = 0, max = 28) missed events per catchment. Under this scenario, median severity again decreased to -7.4 (vs. -6.6 for all reaches) and maximum severity declined further to -85.3 (vs. -75.0), reinforcing the conclusion that reliance on a single monitoring location can lead to substantial underestimation of drought frequency and severity.

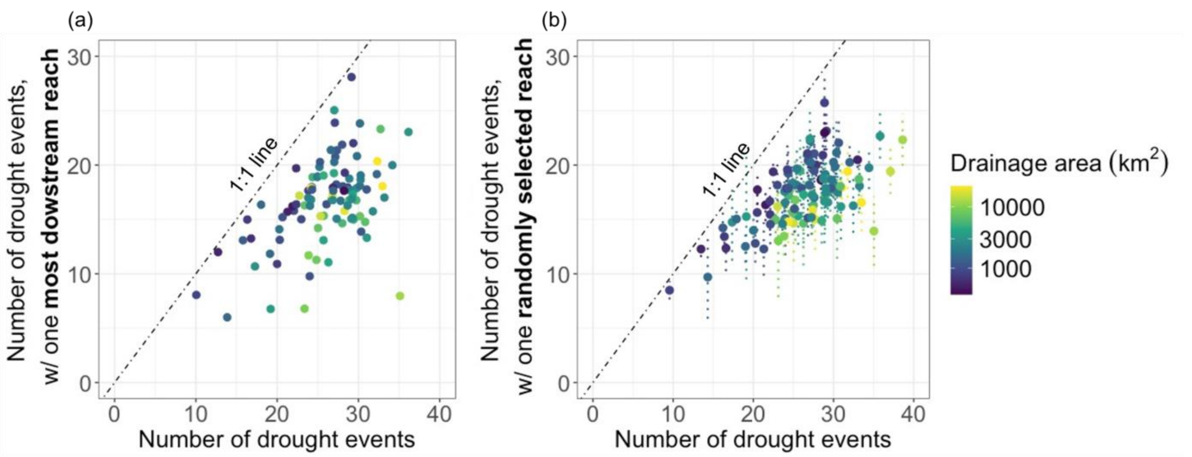

Figure 5. Relationship between the number of drought events identified per catchment when using all the available reaches (X-axis) and when using (a) only the most downstream reach of a catchment or (b) when using a randomly selected reach. In (b), the points and the dotted lines represent the mean and standard deviation of the number of drought events identified from each sampling. The color of the data points represents the catchment drainage area.

https://doi.org/10.5194/egusphere-2025-5783
Preprint. Discussion started: 22 January 2026

By progressively increasing the number of randomly sampled stream reaches per catchment, the theoretical number of stream gauges required to detect all drought events was estimated for each catchment (fig. 6). The drought detection rate, defined as the proportion of detected drought events, increased exponentially with monitoring coverage eventually reaching a plateau when all events were captured. In meso-scale catchments, most events were detected when at least 1 reach per 100 km² of drainage area was included, whereas large-scale catchments required less extensive coverage, with fewer than 0.3 reaches per 100 km² sufficient to detect most events. Reducing this monitoring density by half led to an average of 20 % of events going undetected in large-scale catchments and 15 % in meso-scale catchments. When monitoring density was further reduced to 10 %, approximately 40 % of drought events were missed on average, regardless of catchment size.

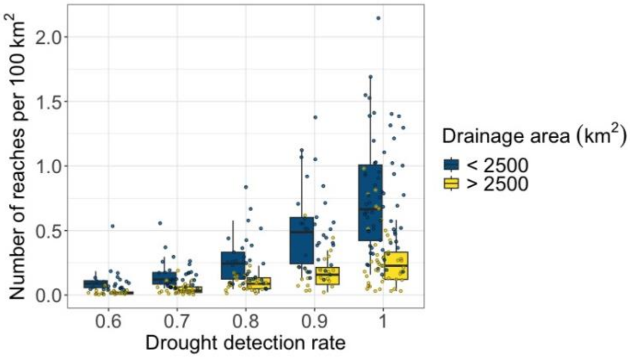

Figure 6. Proportion of catchment-scale drought events detected when using an increasing number of randomly selected reaches. The X-axis (drought detection rate) represents the ratio of drought events detected using a reduced number of reaches to the total number of events detected using all reaches. The Y-axis represents the number of reaches per 100 km^2 of catchment drainage area. The color of boxplots and points represents the total drainage area of catchments in km^2.

4. Discussion

At the continental scale, atmospheric circulation patterns have been shown to explain the simultaneous occurrence of hydrological droughts across catchments (Hannaford et al., 2011). Within the study area, streamflow variability has been linked to large-scale climate drivers such as the North Atlantic Oscillation (NAO) and the Pacific North American (PNA) pattern (Anctil & Coulibaly 2004; Biron et al., 2014). The present study underscores the influence of smaller-scale processes that may interact with these broad atmospheric patterns, as results indicate that hydrological droughts are not always spatially coherent at the catchment scale. While many events (37%) affected more than 90 % of the hydrometric network within a catchment, a notable fraction (14%) remained highly localized, impacting less than 10 % of the hydrometric network (fig. 2).

Overall, the results support the hypothesis that drought severity is positively associated with spatial coherence, with more severe events tending to be more widespread (table 3). Nonetheless, there was still substantial variability in this relationship, and some severe droughts were highly localized. For example, events with severity values lower than the 10th percentile were found to affect less than 10% of a catchment's hydrometric network (fig. 4).

https://doi.org/10.5194/egusphere-2025-5783
Preprint. Discussion started: 22 January 2026

4.1 Strong coupling between meteorological and hydrological droughts may limit spatial coherence in cold, humid catchments

Previous studies have shown that in cold and humid catchments of the eastern United States, hydrological droughts are typically short in duration and closely aligned with meteorological conditions. For example, hydrological droughts in this region are often limited to single year events (Patterson et al., 2013), in contrast to catchments in drier climates, where multi-year droughts are more common due to greater hydrological memory (de Lavenne et al., 2022). Consistent with these results, this study found that the median duration of hydrological drought events remained below 12 months (table 2). Furthermore, in the eastern United States, meteorological and hydrological droughts tend to be of similar duration, with the onset and recovery of hydrological droughts largely controlled by meteorological droughts (Apurv & Cai, 2020).

This strong coupling suggests that spatial variability in precipitation may contribute to within-catchment variability in hydrological drought occurrence. For example, localized rainfall events may alleviate drought conditions in certain stream reaches while other parts of the catchment remain affected, potentially explaining the observed lack of spatial coherence in some drought events. Given the well-established role of climate in governing hydrological drought propagation (Apurv et al., 2017; Van Loon et al., 2014), further research is needed to evaluate how within-catchment spatial variability in drought occurrence differs across climate zones. For example, spatial coherence of hydrological droughts may be greater in dry regions compared to the patterns observed in this study in humid, snowmelt-dominated catchments.

4.2 The influence of catchment properties on drought spatial coherence remains unclear.

This study revealed substantial spatial variability in drought occurrence within catchments. While meteorological factors may contribute to this variability, catchment properties have also been shown to influence the propagation of meteorological droughts into hydrological droughts. Properties of groundwater systems have been linked to the development and persistence of hydrological droughts (Van Lanen et al., 2013). For example, physical characteristics of bedrock, such as lithostratigraphic classes, have been found to explain spatial variability in the baseflow index within the Thames River catchment (16 100 km^2, Bloomfield et al., 2009). Similarly, properties of surface water systems can also influence drought dynamics. In the Savannah River catchment (27 171 km^2, southeastern United States), stream order was a strong predictor of hydrological drought duration (Veettil & Mishra 2020). In contrast, catchment area was not significantly associated with drought duration or severity in the United Kingdom, although it did corelate with the number of events (Barker et al., 2016). Catchment storage capacity has also been shown to influence drought characteristics in cross-catchment studies (Konapala and Mishra 2020, Van Loon and Laaha 2015) and sensitivity analyses (Van Lanen *et al* 2013) and this property may also affect within-catchment variability in hydrological drought.

These findings highlight the need for further research to better understand the drivers of within-catchment variability in hydrological drought occurrence. Improved understanding of local catchment properties that buffer or exacerbate hydrological droughts could improve water resources management and drought forecasting. This need is underscored by our finding that stream reaches not classified as under drought during catchment-scale events were often well above the threshold used to define drought conditions, and even above the historical mean in some cases (fig. 3). This suggests that local conditions may play a critical role in preventing drought occurrence at specific locations within a catchment.

https://doi.org/10.5194/egusphere-2025-5783
Preprint. Discussion started: 22 January 2026

4.3 Single-station data underestimate drought occurrence but accurately represent catchment-scale duration and severity.

Numerous studies have used data from stream gauges to investigate the propagation of meteorological droughts into hydrological droughts across temperate (Barker et al., 2016; Bruno et al., 2022), tropical (Bevacqua et al., 2021; Bhardwaj et al., 2020) and semi-arid (Meresa et al., 2023; Yildirim et al., 2022) climates. These studies commonly rely on a single stream gauge to characterize hydrological droughts within meso-scale (10^2 – 10^3 km^2) or large-scale (10^4 – 10^7 km^2) catchments, often failing to capture within-catchment variability. Moreover, large rivers are disproportionately represented in global hydrometric networks (Krabbenhoft et al., 2022). In contrast, streamflow observations in headwater catchments remain sparse, limiting the ability to assess drought conditions in these smaller, yet widespread and hydrologically important systems.

Findings from this study suggest that accurately capturing all hydrological drought events requires a substantially denser monitoring network than is typically implemented. Specifically, meso-scale catchments (< 2500 km²) would require approximately 1 stream gauge per 100 km², and large-scale catchments (> 2500 km²) about 0.3 stations per 100 km². For example, detecting all events in a 1 000 km² catchment would require roughly 10 stations, while a 10 000 km² catchment would require 30. Achieving a 90 % detection rate would still necessitate ~6 and ~21 stations, respectively, in catchments of these sizes. In contrast, relying on a single gauging station would result in an average detection rate of only 60% in a 1 000 km² catchment and even less in larger ones, reinforcing concerns about underdetection. While this analysis offers a high-level estimate of the monitoring intensity required to detect hydrological droughts, it is likely that more optimal strategies could be implemented (Mishra & Coulibaly, 2009). Given the growing importance of hydrometric networks in monitoring droughts of increasing frequency and severity under climate change, these results highlight the need to explicitly incorporate drought detection objectives into network design. Moreover, hydrological drought assessments should increasingly aim to integrate multiple stream gauges to better capture within-catchment variability. Rather than selecting entirely independent catchments, using nested catchments may offer an effective strategy for monitoring hydrological droughts in cold, humid regions.

Existing hydrometric networks have played a key role in supporting the development of forecasting and early warning systems for droughts (Guo et al., 2020). However, these systems may be biased in cold, humid regions where our results indicate that ~30 % of events may go undetected when relying on a single stream gauge to characterize hydrological droughts (fig. 5a). This underdetection was consistent regardless of the location of the reach location, with a comparable proportion of missed events (35 %, fig. 5b) when reach location was randomly selected within catchments rather than limited to the most downstream reach. While undetected events were typically mild or spatially localized, some were nevertheless severe, underscoring the limitations of using sparse monitoring to capture the full extent of drought conditions.

Despite limitations in capturing all drought events in a catchment with a single stream gauge, our analysis showed that event characteristics such as duration and severity were generally consistent across a catchment. Specifically, the coefficient of variation in drought severity among reaches within the same catchment was relatively low (mean = 16%), indicating strong spatial coherence. As such, while a single station may fail to detect some events, it can still provide a reliable estimate of the severity and duration of those that are detected.

4.4 Limitations

Hydrological drought characterization relied on a robust streamflow reconstruction dataset that nonetheless contains incorporates uncertainty from observations and model hindcasts. The semi-distributed model was calibrated with the KGE’ as an objective function which is well suited for capturing variability in highly seasonal flow regimes such as those found in the study area (Gupta et al., 2009). However, KGE′ is less sensitive to extreme flow values, and may therefore underrepresent flow extremes. The model was calibrated using a regional approach which may reduce performance at the local scale. However, the assimilation of observations into the final streamflow reconstruction dataset helps to mitigate these limitations. Uncertainty in the streamflow reconstruction dataset was thoroughly assessed, with key sources including the density of meteorological and hydrological stations, catchment size and the model's reliance on air temperature and precipitation as input variables (Lachance-Cloutier et al., 2017; Martel et al., 2023). While errors in interpolated data could influence the spatial coherence of hydrological droughts at the catchment scale, this effect is likely limited, as results were consistent across time scales, drought thresholds, and catchments.

The use of streamflow reconstruction allowed for extensive spatial coverage across the study area, enabling a comprehensive assessment of hydrological droughts. Importantly, the dataset provided streamflow time series homogenized both in length (52 years) and period (1970–2022), thereby avoiding biases commonly associated with inconsistencies in data availability when computing standardized indices (Hong et al., 2015; Laimighofer & Laaha 2022). It also minimized uncertainty linked to methodological changes in streamflow measurement over time (Hamilton & Moore 2012). Given the continued scarcity of observed streamflow data, particularly in ungauged or headwater regions, streamflow reconstruction techniques appear a valuable approach to improve understanding of within-catchment variability. Accordingly, streamflow reconstruction datasets are increasingly being used to assess hydrological droughts (Smith *et al* 2019, Laraib *et al* 2024).

5. Conclusion

Many hydrometric networks have experience a steady decline over recent decades (Spence *et al* 2007, Haile *et al* 2022, Vörösmarty *et al* 2001) and this study stressed the importance of monitoring streamflow at multiple locations to accurately assess hydrological droughts in cold, humid regions. Similar to recent studies on flash droughts which highlighted that drought events can be concentrated in time (Christian et al., 2019), this study demonstrated that hydrological droughts can also be concentrated in space. For example, 14 % of hydrological droughts impacted less than 10% of the catchment's hydrometric network. These findings emphasize the need for more work at the sub-catchment scale to better capture spatial variability in drought conditions when managing surface waters. While the spatial extent of droughts is commonly considered in the assessment of meteorological (Sharma & Mujumdar 2017), soil moisture (Sheffield et al., 2009) and groundwater (Tallaksen et al., 2009) droughts, results suggest that this dimension deserves equal attention in the evaluation of streamflow droughts.

CRediT Authorship contribution statement

Gabriel Bastien-Beaudet: Conceptualization; methodology; formal analysis; data curation; visualization; writing – initial original draft; writing – review and editing. **Marc-André Bourgault:** writing – review and editing; funding acquisition. **Audrey Maheu:** Conceptualization; writing – initial original draft; writing – review and editing; funding acquisition.

Declaration of competing interest

The authors declare that they have no known competing financial interests or personal relationships that could have appeared to influence the work reported in this paper.

Funding information

This research was supported by funding from Ouranos (Évolution des sécheresses hydrologiques dans le Québec méridional face aux changements climatiques, 710800) and from the Natural Sciences and Engineering Research Council of Canada (NSERC, Discovery grant awarded to A. Maheu, RGPIN-2018-04199).

Open Research

The findings of this study were produced with data from the Hydroclimatological Atlas of Southern Quebec (MELCCFP, 2023) and the Quebec Hydrographic Network Geobase (MRNF, 2019). All results can be reproduced with processed data available from Bastien-Beaudet et al. (2024), licensed under CC BY 4.0. All data processing and analysis were done with R software environment version 4.3.1 (R Core team, 2016), with libraries specified in the methods and references section. All figures were produced with the "ggplot2" library version 3.5.1 (Wickham et al., 2016), available under the MIT license.

https://doi.org/10.5194/egusphere-2025-5783
Preprint. Discussion started: 22 January 2026

9. References

Allan R P, Barlow M, Byrne M P, Cherchi A, Douville H, Fowler H J, Gan T Y, Pendergrass A G, Rosenfeld D, Swann A L S, Wilcox L J and Zolina O (2020) Advances in understanding large-scale responses of the water cycle to climate change. *Annals of the New York Academy of Sciences*, *1472*, 49–75.

Anctil F and Coulibaly P (2004) Wavelet Analysis of the Interannual Variability in Southern Québec Streamflow *J. Climate*, *17* 163–73.

Apurv, T., Sivapalan, M., & Cai, X. (2017). Understanding the role of climate characteristics in drought propagation. *Water Resources Research*, *53*, 9304–9329. https://doi.org/10.1002/2017WR020629

Apurv T and Cai X 2020 Drought Propagation in Contiguous U.S. Watersheds: A Process-Based Understanding of the Role of Climate and Watershed Properties. *Water Resources Research*, *56(9)*, e2020WR027755. https://doi.org/10.1029/2020WR027755

Barker L J, Hannaford J, Chiverton A and Svensson C 2016 From meteorological to hydrological drought using standardised indicators. *Hydrol. Earth Syst. Sci*., *20*, 2483–505.

Bastien-Beaudet, G. (2024). Quantifying within-catchment spatial variability of hydrological droughts in cold, humid regions (Version 1.0.2) [Dataset]. Zenodo. https://doi.org/10.5281/zenodo.17664777

Bevacqua A G, Chaffe P L B, Chagas V B P and AghaKouchak A (2021) Spatial and temporal patterns of propagation from meteorological to hydrological droughts in Brazil. *Journal of Hydrology*, *603*, 126902.

Bhardwaj K, Shah D, Aadhar S and Mishra V (2020) Propagation of Meteorological to Hydrological Droughts in India. *JGR Atmospheres*, *125*, e2020JD033455.

Biron S, Assani A A, Frenette J-J and Massicotte P (2014) Comparison of Lake Ontario and St. Lawrence River hydrologic droughts and their relationship to climate indices. *Water Resources Research*, *50*, 1396–409.

Bloomfield J P, Allen D J and Griffiths K J (2009) Examining geological controls on baseflow index (BFI) using regression analysis: An illustration from the Thames Basin, UK. *Journal of Hydrology*, *373*, 164–76.

Bond N R, Lake P S and Arthington A H (2008) The impacts of drought on freshwater ecosystems: an Australian perspective. *Hydrobiologia*, *600*, 3–16.

Brooks, M. E., Kristensen, K., van Benthem, K. J., Magnusson, A., Berg, C. W., Nielsen, A., Skaug, H. J., Maechler, M., & Bolker, B. M. (2017). glmmTMB balances speed and flexibility among packages for zero-inflated generalized linear mixed modeling. *The R Journal*, *9*, 378–400. https://doi.org/10.32614/RJ-2017-066

Brunner M I and Chartier-Rescan C (2024) Drought Spatial Extent and Dependence Increase During Drought Propagation From the Atmosphere to the Hydrosphere. *Geophysical Research Letters*, *51*, e2023GL107918.

Bruno G, Avanzi F, Gabellani S, Ferraris L, Cremonese E, Galvagno M and Massari C (2022) Disentangling the role of subsurface storage in the propagation of drought through the hydrological cycle. *Advances in Water Resources*, *169*, 104305.

https://doi.org/10.5194/egusphere-2025-5783
Preprint. Discussion started: 22 January 2026

Christian J I, Basara J B, Otkin J A and Hunt E D (2019) Regional characteristics of flash droughts across the United States. *Environ. Res. Commun.*, *1*, 125004.

Dunn, P. K., & Smyth, G. K. (2005). Series evaluation of Tweedie exponential dispersion models. *Statistics and Computing*, *15*, 267–280. https://doi.org/10.1007/s11222-005-7022-4

Fortin, J. P., Turcotte, R., Massicotte, S., Moussa, R., Fitzback, J., & Villeneuve, J. P. (2001). Distributed watershed model compatible with remote sensing and GIS data. I: Description of model. *Journal of hydrologic engineering*, 6(2), 91-99. https://doi.org/10.1061/(ASCE)1084-0699(2001)6:2(91)

Gesualdo G C, Benso M R, Mendiondo E M and Brunner M I 2024 Spatially Compounding Drought Events in Brazil. *Water Resources Research*, 60, e2023WR036629.

Gudmundsson, L., & Stagge, J. H. (2016). SCI: Standardized climate indices such as SPI, SRI or SPEI. R package version 1.0-2. Retrieved from https://CRAN.R-project.org/package=SCI

Guo Y, Huang S, Huang Q, Leng G, Fang W, Wang L and Wang H (2020) Propagation thresholds of meteorological drought for triggering hydrological drought at various levels. *Science of The Total Environment*, 712, 136502.

Gupta H V, Kling H, Yilmaz K K and Martinez G F (2009) Decomposition of the mean squared error and NSE performance criteria: Implications for improving hydrological modelling. *Journal of Hydrology*, *377*, 80–91.

Haile A T, Asfaw W, Rientjes T and Worako A W (2022) Deterioration of streamflow monitoring in Omo-Gibe basin in Ethiopia. *Hydrological Sciences Journal*, *67*, 1040–53.

Hamilton A S and Moore R D (2012) Quantifying Uncertainty in Streamflow Records. *Canadian Water Resources Journal*, *37*, 3–21.

Hannaford J, Lloyd-Hughes B, Keef C, Parry S and Prudhomme C (2011) Examining the large-scale spatial coherence of European drought using regional indicators of precipitation and streamflow deficit. *Hydrological Processes*, *25*, 1146–62.

Hong X, Guo S, Zhou Y and Xiong L (2015) Uncertainties in assessing hydrological drought using streamflow drought index for the upper Yangtze River basin. *Stoch Environ Res Risk Assess*, *29*, 1235–47.

Kling, H., Fuchs, M., & Paulin, M. (2012). Runoff conditions in the upper Danube basin under an ensemble of climate change scenarios. *Journal of Hydrology*, *424*, 264–277. https://doi.org/10.1016/j.jhydrol.2012.01.010

Konapala G and Mishra A (2020) Quantifying Climate and Catchment Control on Hydrological Drought in the Continental United States. *Water Resources Research*, *56*, e2018WR024620.

Krabbenhoft C A, Allen G H, Lin P, Godsey S E, Allen D C, Burrows R M, DelVecchia A G, Fritz K M, Shanafield M, Burgin A J, Zimmer M A, Datry T, Dodds W K, Jones C N, Mims M C, Franklin C, Hammond J C, Zipper S, Ward A S, Costigan K H, Beck H E and Olden J D (2022) Assessing placement bias of the global river gauge network. *Nature Sustainability*, *5*, 586–92.

Kuiper, N. H. (1960). Tests concerning random points on a circle. *Indagationes Mathematicae (Proceedings)*, *63*, 38–47. https://doi.org/10.1016/S0019-3577(60)80034-5

https://doi.org/10.5194/egusphere-2025-5783
Preprint. Discussion started: 22 January 2026

Lachance-Cloutier S, Turcotte R and Cyr J-F (2017) Combining streamflow observations and hydrologic simulations for the retrospective estimation of daily streamflow for ungauged rivers in southern Quebec (Canada). *Journal of Hydrology*, *550*, 294–306.

Laimighofer J and Laaha G (2022) How standard are standardized drought indices? Uncertainty components for the SPI & SPEI case. *Journal of Hydrology*, *613*, 128385.

Laraib M, Iqbal M, Waseem M, Arshed A B, Sultan U, Khan H U, Rahman A, Abbas K, Shah M A, Javaid S and Tariq M A U R (2024) Natural streamflow reconstruction and quantification of hydrological drought in the Soan River basin, Pakistan. *J American Water Resour Assoc*, *60*, 741–54.

de Lavenne A, Andréassian V, Crochemore L, Lindström G and Arheimer B 2022 Quantifying multi-year hydrological memory with Catchment Forgetting Curves. *Hydrol. Earth Syst. Sci.*, *26*, 2715–32.

Lopez-Nicolas A, Pulido-Velazquez M and Macian-Sorribes H (2017) Economic risk assessment of drought impacts on irrigated agriculture. *Journal of Hydrology*, *550*, 580–9.

Lorenzo-Lacruz J, Morán-Tejeda E, Vicente-Serrano S M and López-Moreno J I (2013) Streamflow droughts in the Iberian Peninsula between 1945 and 2005: spatial and temporal patterns. *Hydrol. Earth Syst. Sci.*, *17*, 119–34.

Lytle D A and Poff N L (2004) Adaptation to natural flow regimes. *Trends in Ecology & Evolution*, 19, 94–100.

Malenfant C, Lavigne, M-P, Mailhot E, El-Housni H, Pelletier-Dumont J, Lachance-Cloutier S. (2022). Atlas hydroclimatique du Québec meridional, 2022 – Rapport technique, Direction de l'hydrologie et de l'hydraulique, Ministère de l'Environnement, de la Lutte contre les changements climatiques, de la Faune et des Parcs (MELCCFP). Retrieved from https://www.cehq.gouv.qc.ca/atlas-hydroclimatique/rapport-atlas-hydroclimatique-2022.pdf

Martel J-L, Arsenault R, Lachance-Cloutier S, Castaneda-Gonzalez M, Turcotte R and Poulin A (2023) Improved historical reconstruction of daily flows and annual maxima in gauged and ungauged basins. *Journal of Hydrology*, 623, 129777.

McKee T B, Doesken N J and Kleist J (1993) The relationship of drought frequency and duration to time scales. In *Proceedings of the 8th Conference on Applied Climatology*, 17(22), 179–183.

[MELCCFP] Ministère de l'Environnement, de la Lutte contre les changements climatiques, de la Faune et des Parcs. (2023). Atlas hydroclimatique du Québec méridional, Séries temporelles de débits (1970-2023). [Dataset]. Retrieved from https://www.cehq.gouv.qc.ca/atlas-hydroclimatique/carte-portrait/index.htm

[MELCCFP] Ministère de l'Environnement, de la Lutte contre les changements climatiques, de la Faune et des Parcs. (2018). Document d'accompagnement de l'Atlas hydroclimatique. Retrieved from https://www.cehq.gouv.qc.ca/atlas-hydroclimatique/doc-accompagnement.pdf

[MELCCFP] Ministère de l'Environnement, de la Lutte contre les changements climatiques, de la Faune et des Parcs. (2012). Normales climatiques 1981-2010. Retrieved from https://www.environnement.gouv.qc.ca/climat/normales/climat-qc.htm

https://doi.org/10.5194/egusphere-2025-5783
Preprint. Discussion started: 22 January 2026

Meresa H, Zhang Y, Tian J and Abrar Faiz M (2023) Understanding the role of catchment and climate characteristics in the propagation of meteorological to hydrological drought. *Journal of Hydrology*, *617*, 128967.

Mosley L M (2015) Drought impacts on the water quality of freshwater systems; review and integration. *Earth-Science Reviews*, 140, 203–14.

[MRNF] Ministère des Ressources naturelles et des Forêts. (2019) Géobase du réseau hydrographique du Québec, version 1.1 [Dataset].. Direction de la référence géographique. https://mrnf.gouv.qc.ca/repertoire-geographique/reseau-hydrographique-grhq/

[NRCan] Natural Resources Canada (2013). *Canadian Digital Elevation Model Product Specifications*. Government technical report, Government of Canada, Natural Resources Canada, Canada Centre for Mapping and Earth observation, Sherbrooke (QC), Canada. Retrieved from https://ftp.geogratis.gc.ca/pub/nrcan_rncan/elevation/cdem_mnec/doc/CDEM_product_specs.pdf

Patterson L A, Lutz B D and Doyle M W (2013) Characterization of Drought in the South Atlantic, United States. *J American Water Resour Assoc*, 49, 1385–97.

Pourmahmoud J, Hashemy Shahdany S M and Roozbahani A (2023) Drought Risk Assessment for Surface Water Distribution Systems in Irrigation Districts. *Water Resour Manage*, *37*, 5325–42.

Prudhomme C, Giuntoli I, Robinson E L, Clark D B, Arnell N W, Dankers R, Fekete B M, Franssen W, Gerten D, Gosling S N, Hagemann S, Hannah D M, Kim H, Masaki Y, Satoh Y, Stacke T, Wada Y and Wisser D (2014) Hydrological droughts in the 21st century, hotspots and uncertainties from a global multimodel ensemble experiment. *Proc. Natl. Acad. Sci.*, 111, 3262–7.

R Core Team. (2016). R: A language and environment for statistical computing (version 4.3.1) [Software]. R Foundation for Statistical Computing, Vienna, Austria. *http://www. R-project. org/*.

Ricard S, Bourdillon R, Roussel D and Turcotte R (2013) Global Calibration of Distributed Hydrological Models for Large-Scale Applications. *J. Hydrol. Eng*., 18, 719–21.

Sharma S and Mujumdar P (2017) Increasing frequency and spatial extent of concurrent meteorological droughts and heatwaves in India, *Scientific Reports*, *7*, 15582.

Sheffield J, Andreadis K M, Wood E F and Lettenmaier D P (2009) Global and Continental Drought in the Second Half of the Twentieth Century: Severity–Area–Duration Analysis and Temporal Variability of Large-Scale Events. *Journal of Climate*, 22, 1962–81.

Simeone C E, Hammond J C, Archfield S A, Broman D, Condon L E, Eldardiry H, Olson C G and Steyaert J C (2024) Declining Reservoir Reliability and Increasing Reservoir Vulnerability: Long-Term Observations Reveal Longer and More Severe Periods of Low Reservoir Storage for Major United States Reservoirs. *Geophysical Research Letters*, 51, e2024GL109476.

Smith K A, Barker L J, Tanguy M, Parry S, Harrigan S, Legg T P, Prudhomme C and Hannaford J (2019) A multi-objective ensemble approach to hydrological modelling in the UK: an application to historic drought reconstruction. *Hydrol. Earth Syst. Sci*., *23*, 3247–68.

https://doi.org/10.5194/egusphere-2025-5783
Preprint. Discussion started: 22 January 2026

Spence C, Saso P and Rausch J (2007) Quantifying the Impact of Hydrometric network Reductions on Regional Streamflow Prediction in Northern Canada. *Canadian Water Resources Journal*, 32, 1–20.

Svensson C, Hannaford J and Prosdocimi I (2017) Statistical distributions for monthly aggregations of precipitation and streamflow in drought indicator applications. *Water Resour. Res*., *53*, 999–1018.

Tallaksen L M, Hisdal H and Lanen H A J V (2009) Space–time modelling of catchment scale drought characteristics. *Journal of Hydrology*, *375*, 363–72

Tanguy M, Chevuturi A, Marchant B P, Mackay J D, Parry S and Hannaford J (2023) How will climate change affect the spatial coherence of streamflow and groundwater droughts in Great Britain? *Environ. Res. Lett.*, *18*, 064048.

Van Lanen H A J, Wanders N, Tallaksen L M and Van Loon A F (2013) Hydrological drought across the world: impact of climate and physical catchment structure. *Hydrol. Earth Syst. Sci*., *17*, 1715–32.

Van Loon A F (2015) Hydrological drought explained. *WIREs Water*, *2*, 359–92.

Van Loon A F and Laaha G (2015) Hydrological drought severity explained by climate and catchment characteristics. *Journal of Hydrology*, 526, 3–14.

Van Loon A F, Tijdeman E, Wanders N, Van Lanen H A J, Teuling A J and Uijlenhoet R (2014) How climate seasonality modifies drought duration and deficit. *JGR Atmospheres*, 119, 4640–56.

Van Vliet M T H, Sheffield J, Wiberg D and Wood E F (2016) Impacts of recent drought and warm years on water resources and electricity supply worldwide. *Environ. Res. Lett*., 11, 124021.

Veettil A V and Mishra A k. (2020) Multiscale hydrological drought analysis: Role of climate, catchment and morphological variables and associated thresholds. *Journal of Hydrology*, 582, 124533.

Vörösmarty C, Askew A, Grabs W, Barry R G, Birkett C, Döll P, Goodison B, Hall A, Jenne R, Kitaev L, Landwehr J, Keeler M, Leavesley G, Schaake J, Strzepek K, Sundarvel S S, Takeuchi K and Webster F (2001) Global water data: A newly endangered species. *EoS Transactions*, *82* 54–8.

Wan W, Zhao J, Popat E, Herbert C and Döll P (2021) Analyzing the Impact of Streamflow Drought on Hydroelectricity Production: A Global-Scale Study. *Water Resources Research*, 57, e2020WR028087.

Wang T, Tu X, Singh V P, Chen X, Lin K, Lai R and Zhou Z (2022) Socioeconomic drought analysis by standardized water supply and demand index under changing environment. *Journal of Cleaner Production*, 347, 131248.

Wickham, H., Chang, W., & Wickham, M. H. (2016). Package 'ggplot2' [Software]. *Create elegant data visualisations using the grammar of graphics. Version*, *2*(1), 1-189.

Wlostowski A N, Jennings K S, Bash R E, Burkhardt J, Wobus C W and Aggett G (2022) Dry landscapes and parched economies: A review of how drought impacts nonagricultural socioeconomic sectors in the US Intermountain West. *WIREs Water*, *9*, e1571.

Wu J, Zhang J, Chen X, Wang Z, Guan T, Zhang X, Li X and Wang G (2024) Hydrological drought life-cycle: Faster onset and recovery in humid than semi-arid basins in China. *Journal of Hydrology*, *644*, 132083.

https://doi.org/10.5194/egusphere-2025-5783
Preprint. Discussion started: 22 January 2026

Yevjevich, V. M. (1967) An objective approach to definitions and investigations of continental hydrologic droughts, 23, 25 p., Fort Collins, CO, USA: Colorado State University.

Yildirim G, Rahman A and Singh V P (2022) Meteorological and hydrological drought hazard, frequency and propagation analysis: A case study in southeast Australia. *Journal of Hydrology: Regional Studies*, *44*, 101229.

Zhou Z, Wang P, Li L, Fu Q, Ding Y, Chen P, Xue P, Wang T and Shi H (2024) Recent development on drought propagation: A comprehensive review. *Journal of Hydrology*, *645*, 132196.

Appendix A - Hydrological drought assessment for additional accumulation periods.

SSI-1

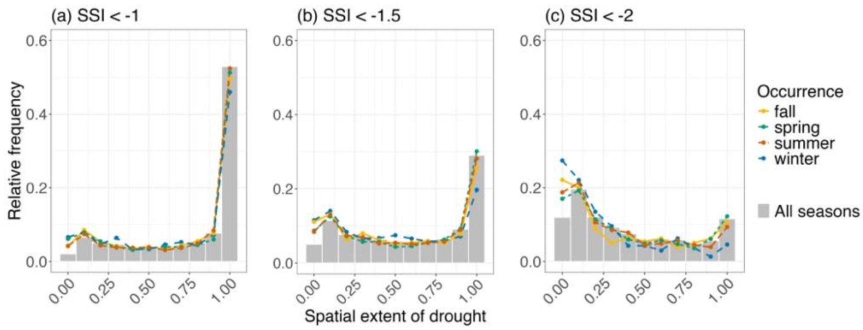

Figure A1. Binned relative frequencies (displayed as both bars and overlaid lines) of the spatial extent of drought events identified with three different thresholds: moderate (SSI < -1), severe (SSI < -1.5) and extreme (SSI < -2). Results are shown for an accumulation period of **one month (SSI-1).** Spatial extent refers to the proportion of the stream network length experiencing drought for a given event. Spatial extent was binned in 11 bins of 0.1 (from 0 to 1) to calculate the relative frequencies of events with different spatial extents. Grey bars represent the entire study area and dotted coloured line refer to the four seasons of drought occurrence (winter = December/January/February, spring = March/April/May, summer = June/July/August, fall = September/October/November).

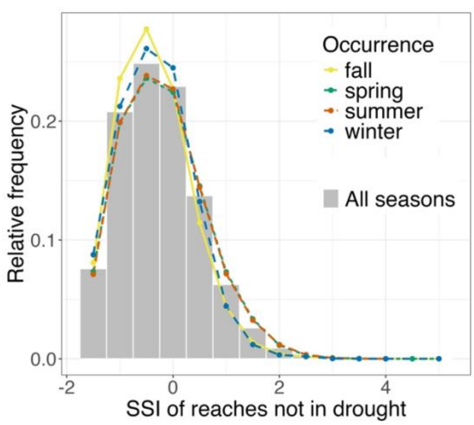

Figure A2. Binned relative frequencies (displayed as both bars and overlaid lines) of the Standardized Streamflow Index (SSI) for reaches that were not in drought during drought events occurring in the catchment. Results are shown for an accumulation period of **one month (SSI-1).** Drought events were identified with the severe threshold (SSI < -1.5). Indices (SSI) were binned in 14 bins of 0.5 (from -1.5 to 5.0) to calculate the relative frequencies of reaches with different SSI values. Grey bars represent the entire study area and dotted coloured line refer to the four seasons of drought occurrence (winter = December/January/February, spring = March/April/May, summer = June/July/August, fall = September/October/November).

https://doi.org/10.5194/egusphere-2025-5783
Preprint. Discussion started: 22 January 2026

SSI-6

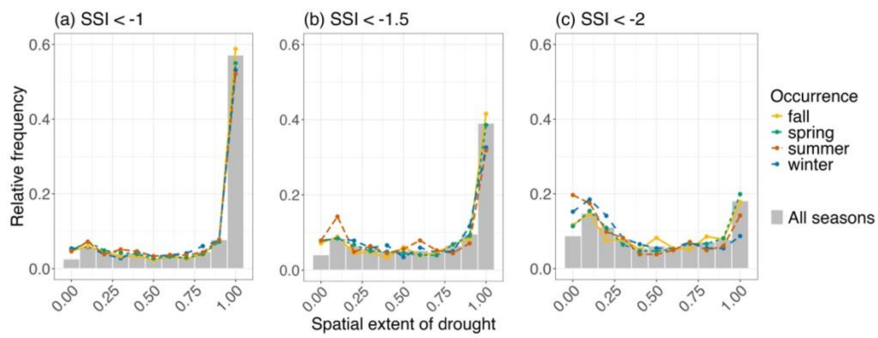

Figure A3. Binned relative frequencies (displayed as both bars and overlaid lines) of the spatial extent of drought events identified with three different thresholds: moderate (SSI < -1), severe (SSI < -1.5) and extreme (SSI < -2). Results are shown for an accumulation period of **six months (SSI-6).** Spatial extent refers to the proportion of the stream network length experiencing drought for a given event. Spatial extent was binned in 11 bins of 0.1 (from 0 to 1) to calculate the relative frequencies of events with different spatial extents. Grey bars represent the entire study area and dotted coloured line refer to the four seasons of drought occurrence (winter = December/January/February, spring = March/April/May, summer = June/July/August, fall = September/October/November).

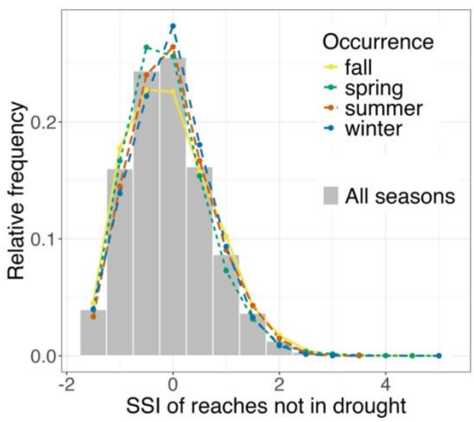

Figure A4. Binned relative frequencies (displayed as both bars and overlaid lines) of the Standardized Streamflow Index (SSI) for reaches that were not in drought during drought events occurring in the catchment. Results are shown for an accumulation period of **six months (SSI-6).** Drought events were identified with the severe threshold (SSI < -1.5). Indices (SSI) were binned in 14 bins of 0.5 (from -1.5 to 5.0) to calculate the relative frequencies of reaches with different SSI values. Grey bars represent the entire study area and dotted coloured line refer to the four seasons of drought occurrence (winter = December/January/February, spring = March/April/May, summer = June/July/August, fall = September/October/November).

https://doi.org/10.5194/egusphere-2025-5783
Preprint. Discussion started: 22 January 2026

Table A1. Annual and seasonal characteristics of catchment-scale hydrological drought events per accumulation period (1, 3, 6 months) and season (winter = December/January/February, spring = March/April/May, summer = June/July/August, fall = September/October/December). CV corresponds to the coefficient of variation.

Occurrence	Accumulation period (months)	Number of droughts per catchment			Duration (months)			Severity (-)			Spatial extent (% of stream length in drought)		
		Median	Mean	CV (%)	Median	Mean	CV (%)	Median	Mean	CV (%)	Median	Mean	CV (%)
All seasons	1	37	37	23	4	5	69	- 4.5	- 5.5	71	59	56	66
	3	27	26	19	7	8	69	- 6.6	- 8.1	74	68	61	60
	6	16	16	20	11	13	73	- 10.3	- 13.4	79	80	65	56
Winter	1	5	6	50	4	4	69	- 3.6	- 4.3	68	48	50	71
	3	5	5	40	6	7	78	- 5.3	- 7.0	81	58	57	65
	6	3	3	54	10	12	78	- 8.6	- 10.7	84	73	62	59
Spring	1	12	12	32	4	5	77	- 4.2	- 5.4	77	67	59	64
	3	9	9	35	6	8	68	- 6.6	- 8.1	70	75	63	59
	6	6	7	33	11	13	73	- 11.0	- 13.9	74	82	65	56
Summer	1	12	12	29	5	6	65	- 5.3	- 6.3	69	62	57	65
	3	7	7	34	7	8	68	- 7.1	- 8.3	73	69	62	59
	6	2	3	54	10	15	76	- 9.7	- 14.6	86	63	59	63
Fall	1	8	8	38	5	5	57	- 5.1	- 5.3	58	55	55	68
	3	6	6	41	7	9	65	- 7.0	- 8.7	72	66	60	61
	6	4	4	50	11	13	67	- 10.8	- 13.6	77	85	68	53

https://doi.org/10.5194/egusphere-2025-5783
Preprint. Discussion started: 22 January 2026

Appendix B - Validation of the linear mixed model

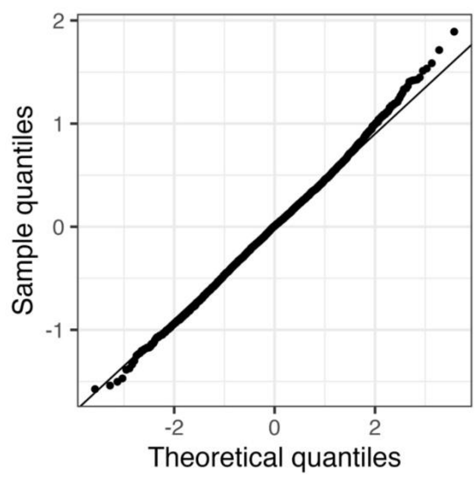

Figure B1. Normal Q-Q plot of the linear mixed model presented in Table 3.

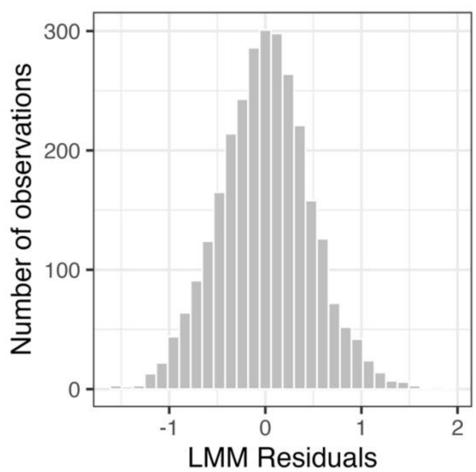

Figure B2. Histogram of residuals of the linear mixed model presented in Table 3.

https://doi.org/10.5194/egusphere-2025-5783
Preprint. Discussion started: 22 January 2026

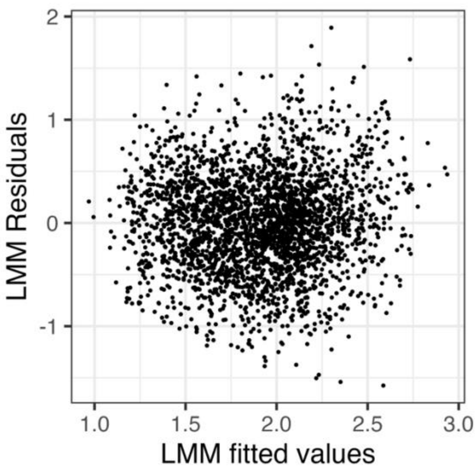

704 **Figure B3.** Residual analysis plot of the linear mixed model presented in Table 3.

https://doi.org/10.5194/egusphere-2025-5783
Preprint. Discussion started: 22 January 2026

Appendix C - Linear mixed models results

Table C1. Estimated regression parameters, standard errors, z-values, p-values and 95% confidence intervals of the linear mixed model for an **accumulation period of 3 months (SSI-3),** with a **moderate threshold (SSI < -1)**. Estimated values of variance (σ) for $\sigma_{catchmentID}$ and σ_{year} are 0.018 and 0.036, respectively. Estimated R^2 value is 0.42. (n = 4124)

	Estimate	95% confidence interval	Std. error	z-value	p-value
(Intercept)	0.522	[0.438, 0.605]	0.042	12.28	< 0.001
Spatial extent	1.229	[1.173, 1.285]	0.028	43.14	< 0.001
Occurrence: Fall	0.185	[0.124, 0.245]	0.031	5.97	< 0.001
Occurrence: Spring	0.109	[0.052, 0.167]	0.029	3.74	< 0.001
Occurrence: Summer	0.214	[0.173, 0.274]	0.031	6.93	< 0.001

Table C2. Estimated regression parameters, standard errors, z-values, p-values and 95% confidence intervals of the linear mixed model for an **accumulation period of 3 months (SSI-3),** with an **extreme threshold (SSI < -2)**. Estimated values of variance (σ) for $\sigma_{catchmentID}$ and σ_{year} are 0.010 and 0.039, respectively. Estimated R^2 value is 0.32. (n = 1707)

	Estimate	95% confidence interval	Std. error	z-value	p-value
(Intercept)	1.825	[1.739, 1.913]	0.045	41.00	< 0.001
Spatial extent	0.523	[0.457, 0.590]	0.034	15.41	< 0.001
Occurrence: Fall	0.193	[0.144, 0.271]	0.040	4.83	< 0.001
Occurrence: Spring	0.159	[0.081, 0.236]	0.040	4.00	< 0.001
Occurrence: Summer	0.167	[0.091, 0.243]	0.039	4.30	< 0.001

Table C3. Estimated regression parameters, standard errors, z-values, p-values and 95% confidence intervals of the linear mixed model an **accumulation period of 1 month (SSI-1),** with a **severe threshold (SSI < -1.5)**. Estimated values of variance (σ) for $\sigma_{catchmentID}$ and σ_{year} are 0.031 and 0.026, respectively. Estimated R^2 value is 0.40. (n = 4061)

	Estimate	95% confidence interval	Std. error	z-value	p-value
(Intercept)	0.919	[0.848, 0.990]	0.036	25.39	< 0.001
Spatial extent	0.764	[0.722, 0.807]	0.022	35.23	< 0.001
Occurrence: Fall	0.223	[0.171, 0.276]	0.027	8.31	< 0.001
Occurrence: Spring	0.131	[0.080, 0.182]	0.026	5.04	< 0.001
Occurrence: Summer	0.278	[0.230, 0.326]	0.025	11.29	< 0.001

https://doi.org/10.5194/egusphere-2025-5783
Preprint. Discussion started: 22 January 2026

Table C4. Estimated regression parameters, standard errors, z-values, p-values and 95% confidence intervals of the linear mixed model for an **accumulation period of 6 months (SSI-6),** with a **severe threshold (SSI < -1.5)**. Estimated values of variance (σ) for $\sigma_{catchmentID}$ and σ_{year} are 0.013 and 0.106, respectively. Estimated R^2 value is 0.48. (n = 1761)

	Estimate	95% confidence interval	Std. error	z-value	p-value
(Intercept)	1.697	[1.578, 1.816]	0.061	28.01	< 0.001
Spatial extent	0.908	[0.836, 0.980]	0.037	24.68	< 0.001
Occurrence: Fall	0.089	[0.008, 0.168]	0.041	2.16	0.0307
Occurrence: Spring	0.078	[-0.0003, 0.155]	0.040	1.96	0.0501
Occurrence: Summer	0.096	[0.002, 0.190]	0.048	2.00	0.0454

https://doi.org/10.5194/egusphere-2025-5783
Preprint. Discussion started: 22 January 2026

Appendix D: Visualization of the two-step process for identifying drought events

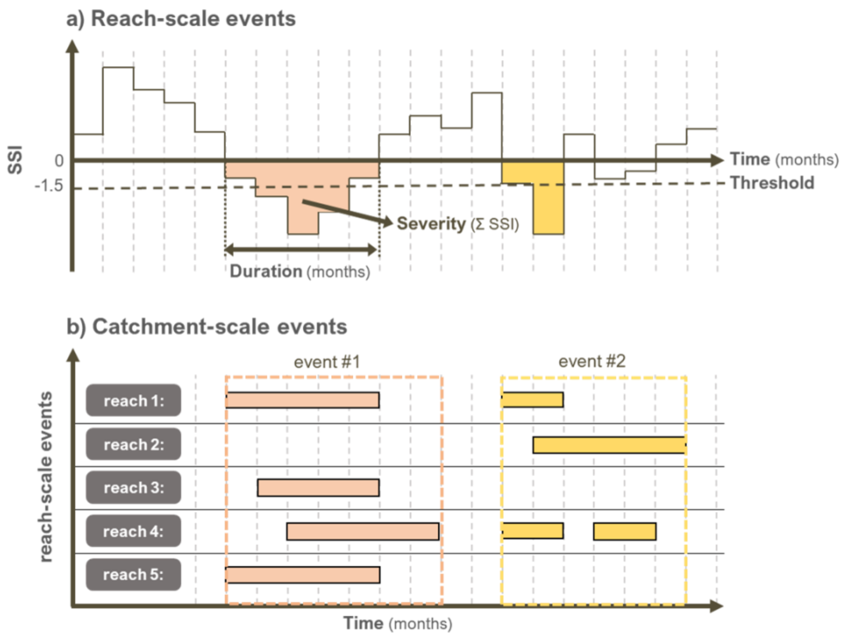

Figure D1. Two-step process for identifying drought events at a) the reach scale (adapted from Zhang et al., 2022) and b) the catchment scale. Panel (a) illustrates how drought events are identified from a time series of the Standardized Streamflow Index (SSI) for reach #1 and characterized by their duration and severity. Panel (b) shows how reach-scale events are aggregated to define catchment-scale events. When multiple events from the same reach were grouped into a single catchment-scale event (event #2, reach 4), their duration and severity were summed. The overall characteristics of each catchment-scale event were calculated as the median values of the corresponding reach-scale events.